The International Journal of Cardiovascular Imaging (2018) 34:1277–1286
https://doi.org/10.1007/s10554-018-1332-2

ORIGINAL PAPER

Precision of regional wall motion estimates from ultra-low-dose cardiac CT using SQUEEZ

Amir Pourmorteza[1] · Noemie Keller[2] · Richard Chen[2] · Albert Lardo[2,3] · Henry Halperin[2,3] · Marcus Y. Chen[4] · Elliot McVeigh[5]

Received: 25 October 2017 / Accepted: 9 March 2018 / Published online: 13 March 2018

Abstract
Resting regional wall motion abnormality (RWMA) has significant prognostic value beyond the findings of computed tomography (CT) coronary angiography. Stretch quantification of endocardial engraved zones (SQUEEZ) has been proposed as a measure of regional cardiac function. The purpose of the work reported here was to determine the effect of lowering the radiation dose on the precision of automatic SQUEEZ assessments of RWMA. Chronic myocardial infarction was created by a 2-h occlusion of the left anterior descending coronary artery in 10 swine (heart rates 80–100, ejection fraction 25–57%). CT was performed 5–11 months post infarct using first-pass contrast enhanced segmented cardiac function scans on a 320-detector row scanner at 80 kVp/500 mA. Images were reconstructed at end diastole and end systole with both filtered back projection and using the "standard" adaptive iterative dose reduction (AIDR) algorithm. For each acquisition, 9 lower dose acquisitions were created. End systolic myocardial function maps were calculated using SQUEEZ for all noise levels and contrast-to-noise ratio (CNR) between the left ventricle blood and myocardium was calculated as a measure of image quality. For acquisitions with CNR > 4, SQUEEZ could be estimated with a precision of ± 0.04 ($p < 0.001$) or 5.7% of its dynamic range. The difference between SQUEEZ values calculated from AIDR and FBP images was not statistically significant. Regional wall motion abnormality can be quantified with good precision from low dose acquisitions, using SQUEEZ, as long as the blood-myocardium CNR stays above 4.

Keywords Myocardial function · CT noise · Wall motion abnormality · Regional cardiac function · SQUEEZ

Introduction

Coronary computed tomography angiography (CCTA) has proven to be an effective test for the assessment of coronary artery disease (CAD). Most recent computed tomography (CT) technologies provide good specificity and sensitivity such that patients with negative or mild non-obstructive CCTA findings do not require further testing and can be safely discharged from the emergency department (ED) [1]. Recent clinical trials have consistently shown the safety, efficiency and cost-savings associated with a negative CCTA to identify patients for discharge from the ED [2]. Furthermore, measuring resting left ventricular (LV) function in the setting of acute pain has been shown to improve the diagnosis of acute coronary syndrome (ACS). Seneviratne et al. demonstrated a 10% increase in sensitivity to detect ACS with the addition of resting regional left ventricular function over coronary assessment alone, leading to significantly improved the overall accuracy [3]. Schlett et al. showed that the addition of regional wall motion abnormality (RWMA) analysis to the CCTA significantly increases the c-statistic in predicting major adverse cardiac events (MACE) [4].

The RWMA analysis has been traditionally performed by visually inspecting 2D movies of the left ventricle or by

✉ Amir Pourmorteza
amir.pourmorteza@emory.edu

1 Department of Radiology and Imaging Sciences, Winship Cancer Insititute, Emory University, Atlanta, GA, USA

2 Department of Biomedical Engineering, Johns Hopkins University School of Medicine, Baltimore, MD, USA

3 Department of Medicine, Johns Hopkins University School of Medicine, Baltimore, MD, USA

4 Advanced Cardiovascular Imaging Laboratory, Cardiopulmonary Branch, National Heart Lung and Blood Institute, National Institutes of Health, Bethesda, MD, USA

5 Departments of Bioengineering, Medicine, and Radiology, University of California San Diego, San Diego, CA, USA

laborious delineation of epi- and endocardial contours of the LV for quantitative wall thickening calculations; however, these techniques are prone to error from through plane motion and require long analysis times. We have previously developed an automatic method for assessment of regional cardiac function called stretch quantification of endocardial engraved zones (SQUEEZ), which is capable of measuring regional endocardial contraction with high spatial resolution in 3D using CT images acquired during a few heartbeats [5, 6]. The method was validated against myocardial strain calculated from tagged MRI in a cohort of large animals [7], and has been utilized clinically to guide electrophysiological interventions [8] and to model personalized blood flow dynamics of the human left atrium [9]. The purpose of this study was to determine the low radiation dose threshold for calculating SQUEEZ with sufficient accuracy and precision to assess regional wall motion abnormalities automatically. The effects of radiation dose reduction on contrast-to-noise ratio (CNR) and the diagnostic image quality has been previously explored in CCTA acquisitions [10, 11]; however, the noise tolerance and spatial resolution requirements are different in CCTA and wall motion analysis. Here we obtained high-fidelity "reference" CT images in animals, and then simulated low-dose acquisitions by creating lower CNR images from the CT projection data using a noise addition tool [12]. Using the same CT projection data as the reference images ensures that the true SQUEEZ values are known exactly, and that the myocardial/blood pool contrast is the same in the lower-fidelity (low-dose, noisier) images. We measured the reduction in precision of SQUEEZ as a function of reducing image quality and radiation dose to determine the threshold for image quality (and therefore the lowest dose) for using SQUEEZ to measure local LV function.

Materials and methods

Animal model

All animal studies were approved by the Johns Hopkins University Institutional Animal Care and Use Committee and were carried out with strict accordance with the Guide for the Care and Use of Laboratory Animals (National Institutes of Health Publication no. 80-23, revised 1985). All efforts were made to minimize suffering. Chronic myocardial infarctions (MI) were created in 10 female swine (weight 35–50 kg, age 12–16 months) raised on a certified farm for experimental animals using a method previously described [5].

To reduce the number of animals involved in this study, we did not create dedicated animal models for this experiment; but instead, we used a cohort that was created for another imaging study and therefore were not euthanized at the end of the CT studies. The animals were acclimated and housed at the animal care center for at least 1 week, followed by 24-h fasting prior to surgery and imaging. Pre-anesthesia sedation was induced by intramuscular injection of Telazol-Ketamine-Xylazine (TKX) cocktail (0.025 ml/kg). Anesthesia was then induced by the injection of Propofol (20 mg/kg) and was sustained by inhaled isoflurane (0.5–2.0%) via endotracheal intubation during surgery or imaging. The pulse rate, respiration, and blood oxygen levels were monitored during the procedures. The left anterior descending (LAD) coronary artery was engaged with a catheter under fluoroscopic guidance. The LAD was occluded just distal to the second diagonal branch by inflating an angioplasty balloon. After 120 min, the occlusion was terminated and the restoration of flow was confirmed by angiography. The CT imaging studies were performed 5–11 month after MI induction.

Image acquisition

The animals received intravenous metoprolol (2–5 mg) and/or amiodarone (50–150 mg) prior to the scan to achieve a heart rate < 100 beats/min. The CT scans were performed using a 320-detector scanner (Aquilion ONE, Toshiba Medical Systems Corporation, Otawara, Japan). After scout acquisitions a 60–100 ml bolus of iodixanol (Visipaque, 320 mg iodine/ml, Amersham Health, Amersham, United Kingdom) was injected intravenously at a rate of 4 ml/s and a first-pass cardiac function scan was performed. The scan was triggered to start when the intensity of the contrast agent in the left ventricle exceeded 200 HU. The high quality breath-hold "reference" CT acquisitions were performed using a 5-beat retrospectively-gated CT protocol with the following parameters: gantry rotation time 350 ms, detector collimation 280 to 320×0.5 mm, and X-ray tube voltage/current of 80 kVp/500 mA. Images were reconstructed every 5% of the R-R interval using the FC08 reconstruction kernel at $0.39 \times 0.39 \times 0.50$ mm^3 voxel size. Two reconstruction algorithms were used: (a) filtered back-projection (FBP) with the standard Toshiba Quantum Denoising Software (QDS+) and (b) the standard setting of Toshiba's Adaptive Iterative Dose Reduction 3D (AIDR 3D) [13]. When necessary, ECG editing was performed to account for arrhythmias. Figure 1 shows a typical outcome of the reconstruction algorithms.

Noise simulation

To simulate the effects of low-dose acquisitions for each scan, eight lower dose acquisitions were simulated using the CT manufacturer supplied noise addition toolbox [12].

The noise simulation toolbox takes high-dose CT projections as input and models scanner-specific photon statistics

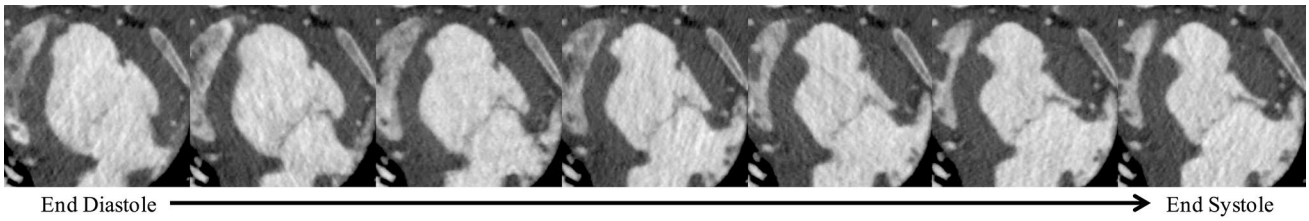

Fig. 1 Typical cardiac CT data used in the study. Multiple phases showing a single axial slice of the 4D reference acquisition used to obtain SQUEEZ (Animal #1 in Table 1). The images were reconstructed with the standard setting of the AIDR3D algorithm

(Poisson distribution) and electronic noise (Gaussian distribution) while taking into account the dynamic range and variance gain of the detector system at different tube currents.

The reference datasets were acquired at tube current–time product of 111–127 mAs. The effective mAs levels of the lower dose simulations were set at the following descending values: 100, 80, 60, 50, 40, 30, 20, 10, and 5. Each simulation was reconstructed using FBP and AIDR3D as described in the previous section. While the noise level in the images will change with mAs, the quality of the images also is dependent on the concentration of X-ray contrast agent in the LV blood pool. Therefore, the LV blood versus myocardium CNR was calculated as a measure of image quality for all reconstructions. Figure 2 shows a sample of the reconstructed reference and noisy images. This series of images produced an LV blood pool signal that could be automatically segmented from the surrounding myocardium using simple intensity thresholding. An expert reader also assessed the image quality to exclude cases with prominent low-dose ring artifacts in the LV, which could not be automatically segmented. Testing CNR sensitivity of SQUEEZ was just one experiment obtained with this set of infarcted swine; other hypotheses were tested with the CT images that are not reported in this paper.

Global function and SQUEEZ

Regional wall motion was calculated by tracking the left ventricular endocardium by segmenting the LV blood from the myocardium and calculating the trajectories of the endocardial features on a dense triangular mesh representing the surface. For each cardiac phase, the bright left ventricle blood pool was extracted using simple automatic thresholding yielding a set of 3D "casts" with the details of the LV endocardium engraved on each cast. The LV blood volume was calculated and phases with maximum and minimum volume were selected as the end-diastole and end-systole, respectively. The global ejection fraction was calculated from the LV volumes.

Next, a 4D non-rigid deformation algorithm was used to warp the end-diastolic triangular mesh on to the shape of the end-systolic mesh in the cardiac cycle. The resulting deformation fields were used to precisely calculate the local wall motion on the triangular mesh. Since the registered meshes have corresponding triangular elements, the regional myocardial function can be expressed as a number reflecting the amount of local stretch on each triangular element of the mesh surface. For each triangle on the end-diastolic mesh, ξ, the triangle's area at end-diastole $A(\xi, t=ED)$, and at later phases $A(\xi,t)$ were computed; the ratio of areas was computed, and the square root was taken to make the dimensions of the metric the same as 1D contraction or stretch: $SQUEEZ(\xi, t) = \sqrt{A(\xi, t)/A(\xi, ED)}$.

For normal muscle, we expect to observe local contraction and for abnormal muscle in the infarct regions we expect either weak/no contraction or local stretch during systole. We call this method "Stretch QUantification of Endocardial Engraved Zones" or SQUEEZ [5]. For example, a local SQUEEZ value of 0.75 means the tissue has contracted 25%, a value of 1.00 means the tissue is static, and a value of 1.25 means the tissue has stretched by 25%. This estimate of deformation is not sensitive to direction.

Our previous studies have shown that chronic infarcts in this animal model caused functional maps that featured regional abnormalities [5]; these patterns of non-uniform function provided important features that SQUEEZ must resolve in order for SQUEEZ to be useful in detecting local abnormalities. In a normal heart, SQUEEZ values are relatively uniform over the LV taking on values of 1.0 at end-diastole through ~0.5 at end-systole; in the infarcted hearts the end-systolic SQUEEZ values typically range from 0.5 (in the normal contracted regions) through 1.2 (in the abnormal stretched regions) [5]. This provided us with a broad spectrum of SQUEEZ values to include in the noise sensitivity analysis.

Effect of decreasing LV blood-myocardium CNR on the precision of SQUEEZ

End-systolic SQUEEZ was calculated as a measure of regional wall motion for all noise levels. For each animal, the SQUEEZ map calculated from the reference image was used as the ground truth for calculating the point-by-point

error in SQUEEZ maps calculated from the images with additional noise.

Effect of reducing spatial resolution on the precision of SQUEEZ

Spatial smoothing is a simple and commonly used method of image noise reduction; therefore, it is possible to acquire very low-dose images to calculate SQUEEZ if smoothing itself does not reduce the precision of the estimates for detecting abnormal wall motion. To this end, we assessed the effect of spatial smoothing on SQUEEZ in noisy acquisitions. For each noise level the 3D CT volumes were smoothed by a series of 3D Gaussian kernels with increasing widths (standard deviations) from $\sigma = 0.5$ to 5 voxels (1 voxel $= 0.39 \times 0.39 \times 0.50$ mm^3). The smoothed 3D data was then used for SQUEEZ analysis.

The unsmoothed original high-fidelity FBP reconstruction was used as the reference and the error was calculated as the difference between the SQUEEZ maps of the unsmoothed reference and those smoothed with Gaussian kernels.

Statistical analysis

Continuous data were expressed as mean ± standard deviation (STD). The distributions of the differences between reference SQUEEZ values and lower dose SQUEEZ values were tested for normality using the Lilliefors test [14]. Significance of the differences between the means and standard deviations of variables were tested using the Student's *t* test and the F-test, respectively. White's test was used to investigate heteroscedasticity of differences with respect to SQUEEZ values.

Results

The contrast-to-noise ratio (CNR) between the LV blood and the myocardial tissue was calculated for the reference images and images with added noise (Table 1). The LV blood pool vs. myocardium CNR and the image quality visibly decreased as the simulated current–time product was decreased as seen in Fig. 2. The LV blood in images with blood-myocardium CNR > 4 could be automatically segmented. An expert reader assessed all images; images with unrecognizable blood-myocardium boundaries because of

Table 1 Image CNR

Subject	Recon	Full dose	100 mAs	80 mAs	60 mAs	50 mAs	40 mAs	30 mAs	20 mAs	10 mAs	5 mAs
Animal 1	FBP	25.7	24.2	21.6	21.2	17.9	16.5	14.0	11.8	7.0	3.3
	AIDR	29.4	30.6	28.4	28.4	26.5	25.6	24.7	23.6	15.9	5.8
Animal 2	FBP	8.6	6.4	5.6	4.6	4.8	3.3	2.8	2.1	1.1	0.7
	AIDR	14.6	11.5	9.8	8.5	8.6	6.9	6.2	5.1	3.5	3.2
Animal 3	FBP	6.6	5.7	5.4	4.9	4.0	3.8	3.3	2.4	0.4	0.0
	AIDR	8.4	8.1	8.1	7.7	6.9	6.7	6.0	4.7	1.6	0.0
Animal 4	FBP	10.4	10.1	9.2	9.0	8.3	8.1	6.8	5.3	2.9	1.4
	AIDR	11.7	11.7	11.3	11.5	11.1	11.5	11.3	9.9	6.3	2.6
Animal 5	FBP	9.2	8.4	8.1	6.9	6.5	6.1	5.2	3.9	2.2	1.9
	AIDR	13.0	13.1	13.0	12.9	12.7	13.3	12.4	9.2	5.4	5.9
Animal 6	FBP	11.2	10.4	9.2	8.9	8.9	7.5	7.2	6.6	3.7	1.6
	AIDR	12.5	12.4	11.7	12.4	11.9	11.2	11.6	11.7	7.3	3.4
Animal 7	FBP	14.3	12.8	10.7	10.0	10.6	8.2	6.9	6.2	4.7	1.8
	AIDR	18.3	19.2	16.1	16.1	19.3	15.6	15.7	16.4	15.5	5.4
Animal 8	FBP	18.5	17.1	17.5	15.6	15.6	15.3	13.3	10.3	8.0	4.9
	AIDR	19.9	19.5	20.9	19.5	19.9	19.8	19.4	18.2	18.8	15.8
Animal 9	FBP	4.1	4.0	3.8	3.7	3.1	3.1	2.5	1.8	0.4	1.0
	AIDR	8.5	8.6	8.5	8.4	6.8	7.2	6.3	4.3	1.2	2.6
Animal 10	FBP	22.3	19.1	16.9	15.0	13.3	12.5	9.6	8.4	5.0	3.2
	AIDR	32.8	32.0	32.0	32.8	29.5	29.7	25.6	22.2	11.7	6.4

LV blood pool versus myocardium CNR values for the reference images ("full dose" column) and lower CNR images after addition of noise with the noise tool software

Each column gives the mAs value used in the noise simulation tool

FBP filtered back-projection, *AIDR* adaptive iterative dose reduction

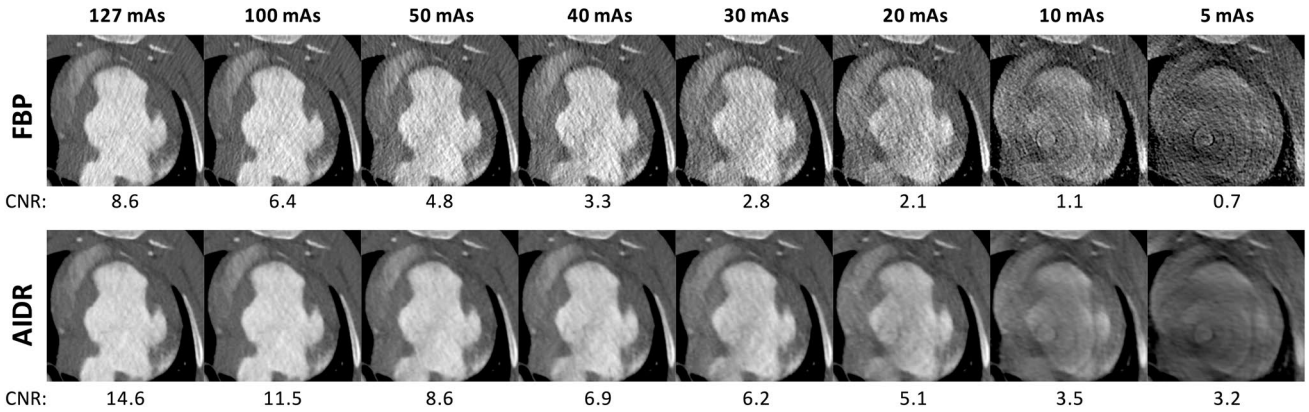

Fig. 2 Original and noisy data reconstructed with two algorithms. The original reference images (left column, 127 mAs) compared with images at lower mAs values created from the same projection data after the addition of noise for Animal #2 in Table 1. Top row images reconstructed with FBP; Bottom row images reconstructed with AIDR3D standard setting. Low-dose ring artifacts are visible at 20 mAs and are very prominent at 10 and 5 mAs. *FBP* filtered back-projection, *AIDR* adaptive iterative dose reduction

increased image noise and artifact were excluded from the study. The inferior image quality in the excluded cases could be attributed to the presence of low-dose ring artifacts in the images. The images containing these artifacts included all of the 5, 10, and five of the 20 mAs simulations (see Fig. 2). A total of 74 cases (over 10 animals) were used in the SQUEEZ analysis.

Global ejection fraction percentages for each of the ten animals were calculated from the 3D blood casts of the LV at end diastole and end systole. The average ejection fraction (EF) was 43 ± 12% and the average heart rate was 74 ± 13 bpm. The range of SQUEEZ values observed in the animals was 0.5 (normal contraction) through 1.2 (stretch in the infarct zone).

Dependence of SQUEEZ precision on image noise level

Figure 3 shows the SQUEEZ plots obtained from images with decreasing mAs values (and also decreasing CNR) in one animal (Animal 4 from Table 1). These plots are in the classic bulls-eye format used in functional cardiac imaging. We calculated the error in SQUEEZ due to the simulated noise using the full-dose FBP reconstruction as the reference (Fig. 3a, 111 mAs, shown in a red box). The standard deviation of the error for both FBP and AIDR reconstructions increased as the simulated mAs values decreased. We did not find a statistically significant difference in standard deviation of error (precision) with respect to the value of SQUEEZ i.e. the precision was not heteroscedastic. The slight difference between the noisy AIDR and FBP SQUEEZ maps can be attributed to the smoother texture of AIDR images which leads to a smoother endocardial mesh. This effect is described in detail in "Dependence of SQUEEZ precision on spatial smoothing" section.

The main result of this study is shown in Fig. 4 where the standard deviation of the error in SQUEEZ as a function of decreasing CNR in the lower dose images is plotted for all end-systolic images in all animals; the images with too much ring artifact were excluded from the analysis as previously explained. These results indicate that for acquisitions with blood-myocardium CNR > 4, SQUEEZ can be estimated with maximum STD error of ± 0.04 ($p < 0.001$). The low-dose SQUEEZ maps calculated from AIDR reconstructions seem to show slower deterioration as the CNR decreases compared to the FBP SQUEEZ maps; however, this difference was not statistically significant.

Dependence of SQUEEZ precision on spatial smoothing

The error in the SQUEEZ maps was calculated using the original unsmoothed highest dose FBP reconstruction as the reference (Fig. 5). A Lilliefors test ($\alpha = 0.001$) confirmed the normal distribution of the error distributions.

For these data, the $\sigma = 1$ kernel provided the optimal spatial smoothing for obtaining maximum precision in SQUEEZ as shown in Fig. 6. The precision of SQUEEZ monotonically decreased for sigma values greater than the optimal sigma; however, the resultant increase in error of the SQUEEZ map remained below 0.06 for $\sigma \leq 5$ pixels.

The precision of SQUEEZ from the unsmoothed AIDR images was identical to the $\sigma = 1$ data for the smoothed FBP reconstructed images (Fig. 6). This would indicate that the AIDR reconstruction produced images that contained inherent smoothing. The standard deviation of error in AIDR unsmoothed volumes and volumes with $\sigma = 1$ were not significantly different, suggesting that the "effective" spatial smoothing of standard AIDR is the same as the spatial smoothing of a Gaussian kernel with $\sigma = 1$. Furthermore,

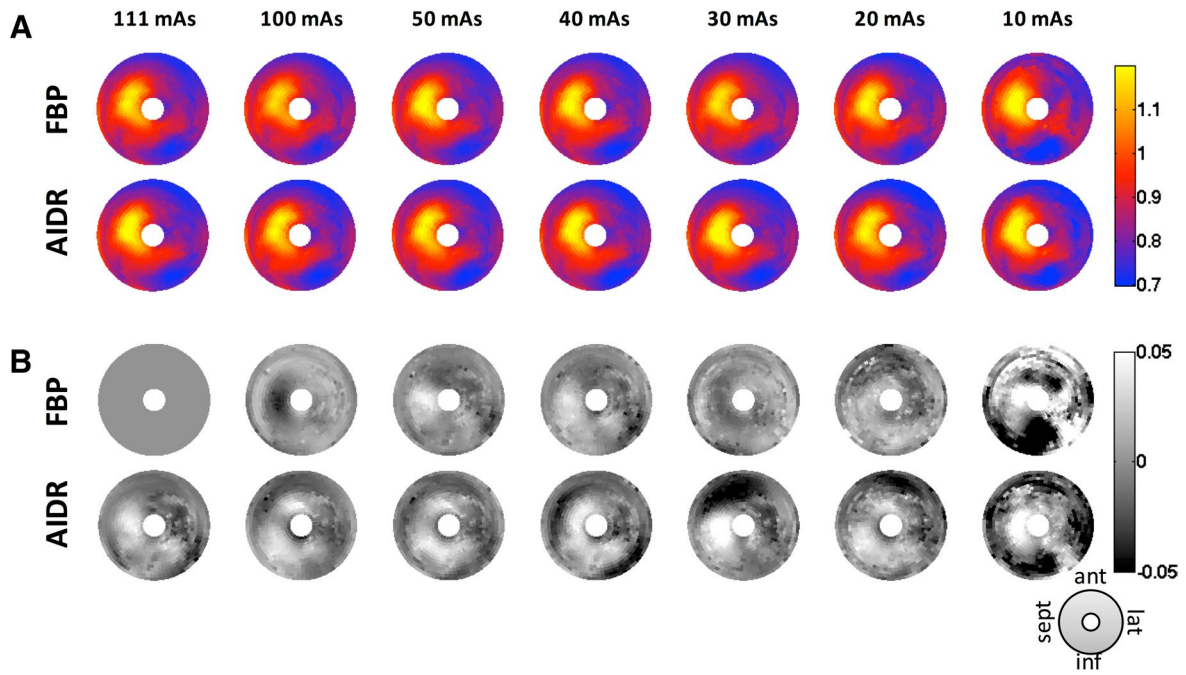

Fig. 3 SQUEEZ maps at increasing noise levels. SQUEEZ plots **a** End-systolic SQUEEZ plots in one animal (#4 in Table 1) obtained from the reference image (top left) and noise images with decreasing mAs, and decreasing CNR. The SQUEEZ plot in the top left corner (FBP, 111mAs) was used as the "reference". **b** Maps showing the difference in SQUEEZ values between the lower CNR images and the reference SQUEEZ plot. The standard deviation of the error for both FBP and AIDR reconstructions increased as the simulated mAs values decreased. The difference between the noisy AIDR and FBP SQUEEZ maps can be attributed to the smoother texture of AIDR images which leads to a smoother endocardial mesh. *SQUEEZ* stretch quantifier of endocardial engraved zone

the STD of error for FBP volumes smoothed with $\sigma = 1$ was not significantly different from that of unsmoothed AIDR volumes.

Discussion

In this paper, we have presented the precision of SQUEEZ in low-fidelity images as would be obtained with low-dose acquisitions for the assessment of regional wall motion abnormalities. Cardiac CT images from wide detector scanners have complex noise properties due to the cone-beam reconstruction. The new iterative reconstruction techniques also introduce correlations in image noise that are not easily simulated without access to proprietary reconstruction and calibration techniques; we obtained these techniques from the manufacturer for this study. In this paper, when possible, we used the high-fidelity (high-dose, low-noise, and low-artifact) images reconstructed with FBP as the reference ground truth for the evaluation of SQUEEZ precision in noisy images.

We used animals in this study so that the radiation dose from the high-fidelity scans would not be a health concern. We selected a myocardial infarction model to create a wide dynamic range of myocardial function in each heart, which included contraction and stretch in different regions of the same heart. It should be noted that this animal model was not created solely for the purpose of the present study; it was part of a larger longitudinal study on myocardial infarction. Therefore, it was not possible to compare the results of CT SQUEEZ to the gold standard measurements such as delayed contrast enhanced MRI, myocardial strain calculated from tagged MRI, or post-mortem histological analysis; this is a limitation of the current study, although such validations have been reported in other cohorts [5, 7].

Even in animal models, consecutive scans may be slightly different due to respiratory motion, the variability in heart rate, stroke volume, and X-ray contrast agent concentration. Therefore, we created the noisy images by adding different levels of noise to the projection data of a high-fidelity acquisition; this ensured that the underlying SQUEEZ data was identical.

The high-fidelity reference datasets were acquired at 80 kVp to maximize the soft tissue vs. iodinated contrast agent contrast with a high tube current of 500 mA to ensure a very low-noise image without overheating the tube. This resulted in tube current–time products in the 111–127 mAs range; the different mAs values can be attributed to slightly different scan times due to different heart rates of the animals.

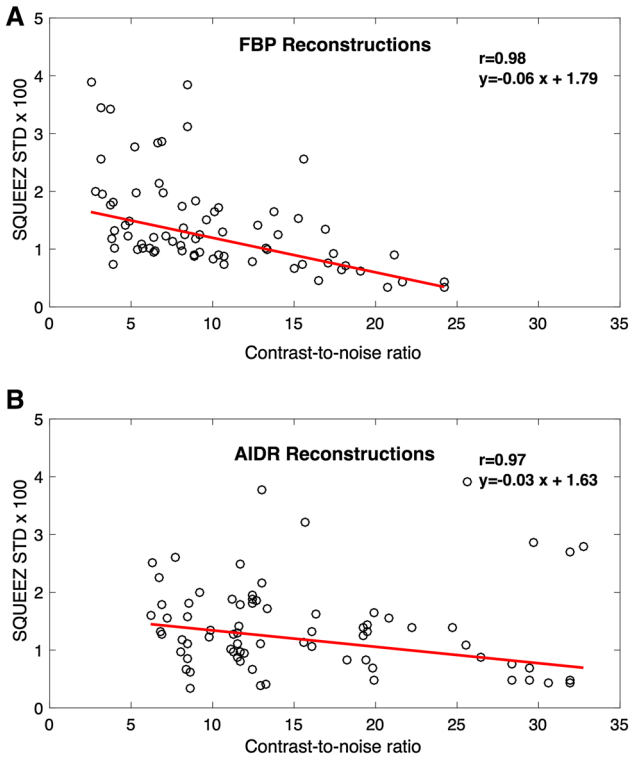

Fig. 4 SQUEEZ error vs. contrast-to-noise ratio. Standard deviation of error in SQUEEZ vs. CNR between the LV blood and myocardium for images reconstructed with FBP (**a**) and AIDR 3D (**b**) for simulated acquisitions (20–100 mAs) over all 10 animals (N = 74); images with unrecognizable blood-myocardium border due to excessive ring artifact were excluded. These results indicate that for acquisitions with blood-myocardium CNR > 4, SQUEEZ can be estimated with a precision of ±0.04 ($p < 0.001$). The low-dose SQUEEZ maps calculated from AIDR reconstructions seem to show slower deterioration as the CNR decreases compared to the FBP SQUEEZ maps; however, this difference was not statistically significant. *FBP* filtered back-projection, *AIDR* adaptive iterative dose reduction, *SQUEEZ* stretch quantifier of endocardial engraved zone, *STD* standard deviation

A high contrast-to-noise ratio (CNR) between the LV blood pool signal and the myocardium is the primary factor for robust automatic segmentation of the LV blood pool. The highest CNR values were approximately 30, and the lowest values were approximately 1 in images that had recognizable features. The difference in the CNR values in the reference images was due to differences in X-ray contrast concentration in the LV blood pool at the time of image acquisition; this could be attributed to difference in the ejection fraction of different animals, since the contrast injection protocol remained unchanged throughout the study.

LV volumes of noisy acquisitions with CNR > 4 between the blood pool and the myocardium could be used to estimate SQUEEZ. In these cases, maximum STD of error in SQUEEZ due to noise was ±0.04. Therefore, it is safe to assume that SQUEEZ can be estimated from noisy images with precision of ±0.04. Based on the current results and previous studies of SQUEEZ in acute [7] and chronic [5] myocardial infarct models, the typical dynamic range of SQUEEZ is approximately 0.7 (from 0.5 to 1.2). Typical SQUEEZ values in the heart range from 0.5 in normal contracting tissue, through 1.0 in akinetic tissue, to 1.2 in diseased tissue that undergoes paradoxical stretching during systole. Hence, the ±0.04 error represents a relatively high precision (0.04/0.7 = 5.7%) for detection of LV function.

The results also suggest that increasing CNR can improve the precision of SQUEEZ (Fig. 4). The CNR may be increased by increasing the amount of X-ray contrast agent in the LV blood pool, increasing the radiation dose, reducing the kVp, or all of the above. Also, the CNR can be optimized by careful timing of the scan with respect to the arrival of the iodinated contrast agent bolus into the LV. In addition, most modern CT scanners have built-in applications (under various vendor-specific names), which given a specific target CNR and a topogram of the patient, recommend mAs and kVp values to reach the desired CNR. The scan settings are patient-specific and rely on variables such as weight, height, body shape, and heart rate.

There are at least two possible ways to augment a typical CTA protocol with SQUEEZ:

1. Acquire a separate cine CT scan for SQUEEZ after CTA acquisition: This has the benefit that the tube current, kVp, and other scan parameters of the SQUEEZ scan can be set independently from the CTA scan. The SQUEEZ scan may be performed after a new contrast injection or a prolonged injection trailing from the initial CTA scan. However, in our experience the recirculated contrast agent 1–2 min after the initial CTA scan provides sufficient contrast between blood and myocardium. Yet, in order to maintain the CNR above 4, the radiation dose may need to be increased. This scan protocol has been successfully used to calculate SQUEEZ in previous studies [5–7].
2. Acquire a tube current-modulated cine scan, at a fixed kVp, with the high-mAs phase coinciding with the CTA acquisition (typically 65–75% of the R–R cycle) and reduced mAs elsewhere: This simplifies the clinical workflow and does not require timing and setup of a second cine scan. The advantage of this method is that it eliminates the need for a new contrast injection, and that it provides registered maps of CTA and SQUEEZ. However, the tube current modulation is slow and takes time to ramp up and down. Furthermore, most scanners do not allow the tube current to go below 10% of the maximum current or to be acquired using multi-beat scans. Therefore, the dose modulated scans are not as dose-efficient as separate dedicated low-dose cine CT. This scan protocol has been successfully used to calculate SQUEEZ in a cohort of patients [8, 15]. The deci-

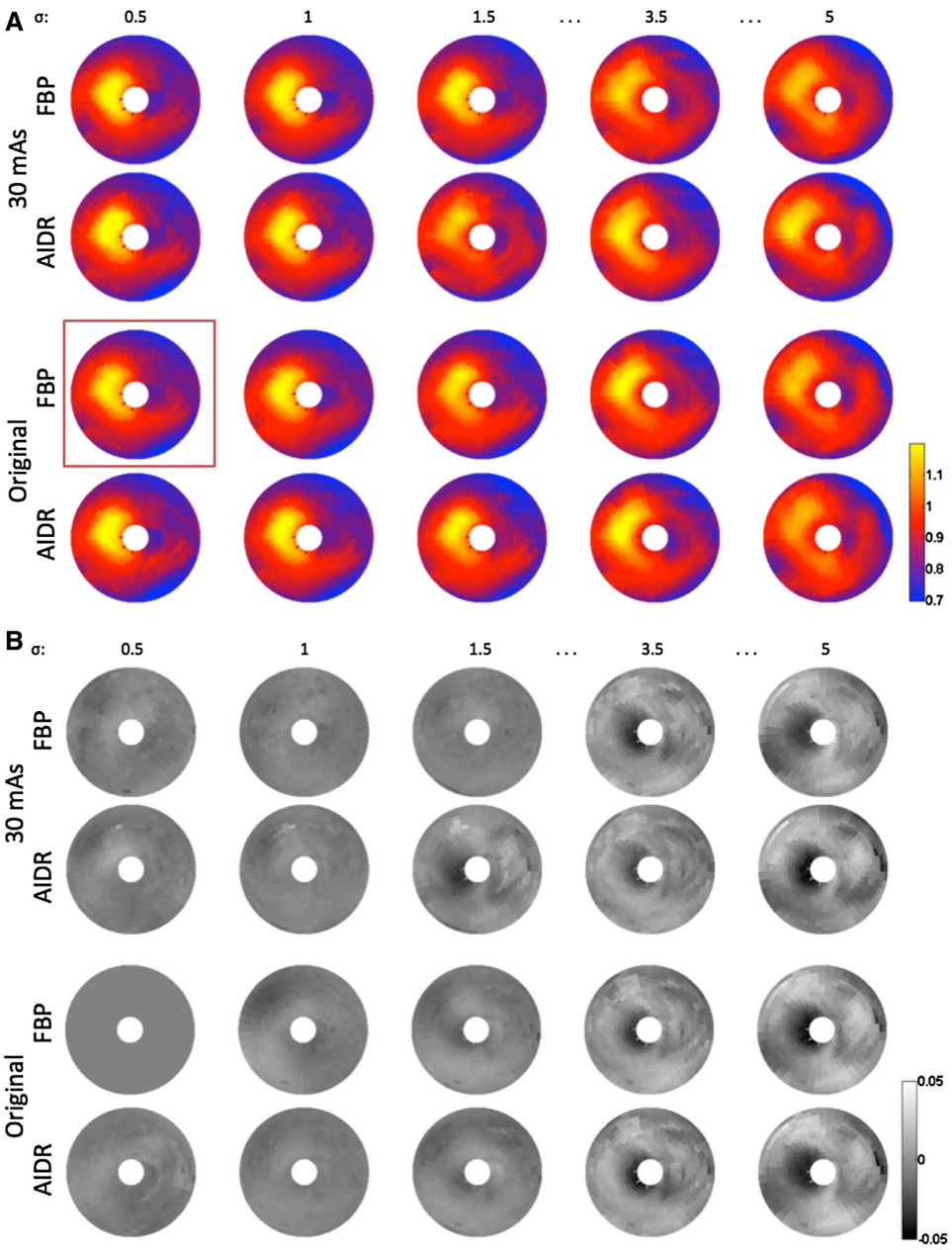

Fig. 5 Effects of spatial smoothing on SQUEEZ maps. **a** SQUEEZ plots obtained for one animal (#5 in Table 1) from images with noise equivalent to a 30 mAs acquisition (top two rows) vs. the original high-dose acquisitions (~120 mAs) (bottom two rows) as the width of the Gaussian smoothing kernel was increased. **b** Error in SQUEEZ with respect to the full-dose FBP acquisition. *FBP* filtered back-projection, *AIDR* adaptive iterative dose reduction, *SQUEEZ* stretch quantifier of endocardial engraved zone

sion on how to augment SQUEEZ into CTA protocol is task-specific and depends on the end goal of the study and the clinical scan workflow.

At very low radiation dose, image quality can be compromised by the presence of ring artifacts [16] (Fig. 2) caused by mis-calibrated or defective detector elements or by photon starvation. Although it is theoretically possible to reduce ring artifacts by careful recalibration of the scanner, most commercial scanners cannot be easily calibrated for mAs levels below 10. This imposes a lower bound for dose reduction by tube current reduction in SQUEEZ with the current technology. However, we believe current CT technology can produce images with sufficient fidelity to apply SQUEEZ at radiation doses comparable to or smaller than the low-dose coronary CTA; There are recent reports of <0.1 mSv CTA scans acquired at 50 mAs and 100 kVp [17].

Here we obtained scan with settings of ~30 mAs and 80 kVp; switching from 100 to 80 kVp alone can reduce the radiation dose by ~35% but in turn may increase the image noise by roughly 25% [18]. This level of noise may render the images nondiagnostic for CTA analysis; however, according to our results the SQUEEZ values calculated from them will have a precision better than 5.7%. This leads us to recommend a tube current modulation in which end-diastolic

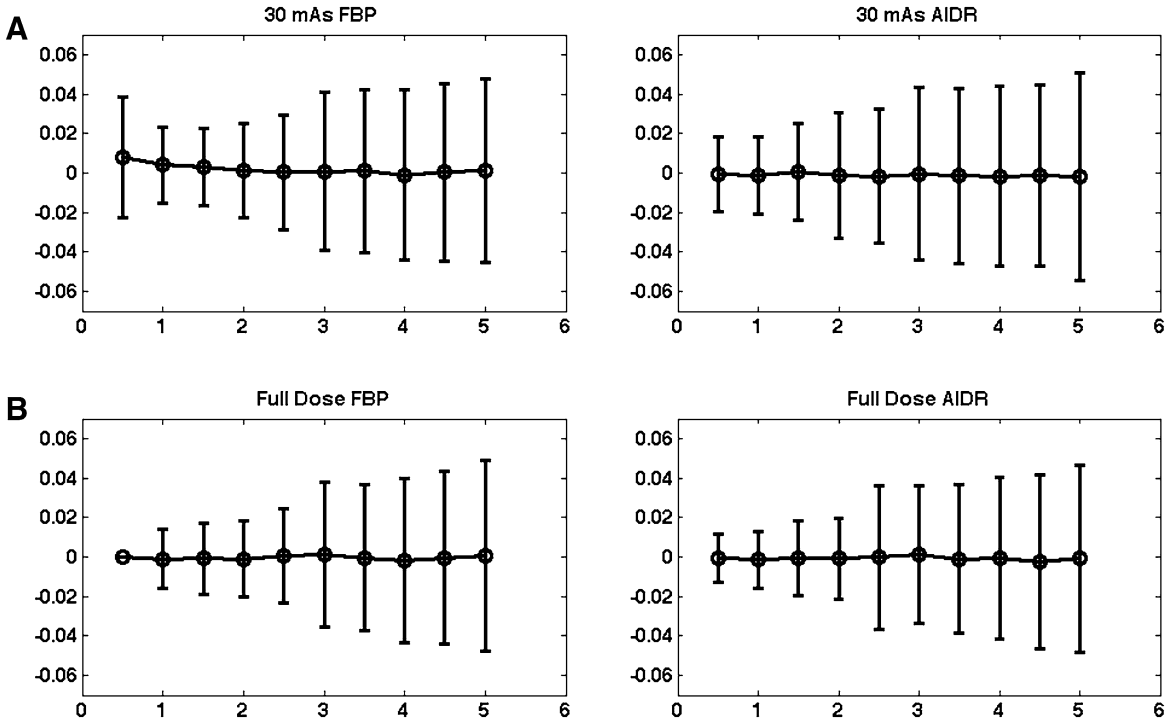

Fig. 6 SQUEEZ error vs. spatial smoothing. Error in SQUEEZ values between the reference (unsmoothed full-dose FBP) and the smoothed volumes reconstructed with FBP and AIDR, for the 30 mAs noisy images (**a**) and the full dose acquisitions (**b**)

images have higher tube current and end-systolic images have lower tube current.

Conclusion

If the LV blood-myocardium CNR is greater than 4, SQUEEZ can assess regional wall motion abnormality with minimal user input with a precision of ± 0.04 (representing 5.7% of the dynamic range of SQUEEZ values [0.5–1.2]). In the absence of ring artifacts, reliable SQUEEZ values were estimated from images with tube current–time values as low as 20 mAs and a radiation dose reduction of a factor of 5–6 over the 111–127 mAs original reference acquisitions. We conclude that accurate quantitative wall motion estimates can be achieved with additional images that will introduce a very small increase in total dose over that used for standard coronary CT angiography.

Funding Funding was provided by National Institutes of Health (Grant Nos. R01-HL64795, R01-HL094610).

Compliance with ethical standards

Conflict of interest AP and EM have a patent application for SQUEEZ (US 14/350,991). MYC receives institutional research support from Toshiba Medical Systems. Other authors did not report any conflicts.

References

1. Cury RC, Feuchtner GM, Batlle JC et al (2013) Triage of patients presenting with chest pain to the emergency department: implementation of coronary CT angiography in a large urban health care system. AJR Am J Roentgenol 200:57–65. https://doi.org/10.2214/AJR.12.8808
2. Cury RC, Budoff M, Taylor AJ (2013) Coronary CT angiography versus standard of care for assessment of chest pain in the emergency department. J Cardiovasc Comput Tomogr 7:79–82. https://doi.org/10.1016/j.jcct.2013.01.009
3. Seneviratne SK, Truong QA, Bamberg F et al (2010) Incremental diagnostic value of regional left ventricular function over coronary assessment by cardiac computed tomography for the detection of acute coronary syndrome in patients with acute chest pain: from the ROMICAT trial. Circ Cardiovasc Imaging 3:375–383. https://doi.org/10.1161/CIRCIMAGING.109.892638
4. Schlett CL, Banerji D, Siegel E et al (2011) Prognostic value of CT angiography for major adverse cardiac events in patients with acute chest pain from the emergency department: 2-year outcomes of the ROMICAT trial. JACC Cardiovasc Imaging 4:481–491. https://doi.org/10.1016/j.jcmg.2010.12.008
5. Pourmorteza A, Schuleri KH, Herzka DA et al (2012) A new method for cardiac computed tomography regional function assessment: stretch quantifier for endocardial engraved zones (SQUEEZ). Circ Cardiovasc Imaging 5:243–250. https://doi.org/10.1161/CIRCIMAGING.111.970061
6. Pourmorteza A, Schuleri KH, Herzka DA et al (2012) Regional cardiac function assessment in 4D CT: comparison between SQUEEZ and ejection fraction. In: 2012 annual international conference of the IEEE engineering in medicine and biology society (EMBC), pp 4966–4969. https://doi.org/10.1109/EMBC.2012.6347107

7. Pourmorteza A, Chen MY, van der Pals J et al (2016) Correlation of CT-based regional cardiac function (SQUEEZ) with myocardial strain calculated from tagged MRI: an experimental study. Int J Cardiovasc Imaging 32:817–823. https://doi.org/10.1007/s10554-015-0831-7
8. Behar JM, Rajani R, Pourmorteza A et al (2017) Comprehensive use of cardiac computed tomography to guide left ventricular lead placement in cardiac resynchronization therapy. Hear Rhythm. https://doi.org/10.1016/j.hrthm.2017.04.041
9. Otani T, Al-Issa A, Pourmorteza A, McVeigh ER, Wada S, Ashikaga H (2016) A computational framework for personalized blood flow analysis in the human left atrium. Ann Biomed Eng 44:3284
10. Hou Y, Ma Y, Fan W et al (2014) Diagnostic accuracy of low-dose 256-slice multi-detector coronary CT angiography using iterative reconstruction in patients with suspected coronary artery disease. Eur Radiol 24:3–11. https://doi.org/10.1007/s00330-013-2969-9
11. Hou Y, Xu S, Guo W et al (2012) The optimal dose reduction level using iterative reconstruction with prospective ECG-triggered coronary CTA using 256-slice MDCT. Eur J Radiol 81:3905–3911
12. Fan Y, Zamyatin AA, Nakanishi S (2012) Noise simulation for low-dose computed tomography. IEEE nuclear science symposium and medical imaging conference (NSS/MIC), pp 3641–3643. https://doi.org/10.1109/NSSMIC.2012.6551836
13. Angel E (Toshiba America Medical Systems I AIDR3D Whitepaper. http://medical.toshiba.com/downloads/aidr-3d-wp-aidr-3d
14. Lilliefors HW (1967) On the Kolmogorov-Smirnov test for normality with mean and variance unknown. J Am Stat Assoc 62:399–402. https://doi.org/10.1080/01621459.1967.10482916
15. Behar JM, Pourmorteza A, McVeigh E, Niederer S, Claridge S, Jackson T, Sohal M, Preston R, Carr-White G, Razavi R, Rajani R, CAR (2015) Cardiac computed tomography is a feasible imaging modality for pre procedural planning in patients undergoing upgrade from pacemakers to CRT. Europace 17:v10–v13
16. Boas FE, Fleischmann D (2012) CT artifacts: causes and reduction techniques. Imaging Med 4:229–240. https://doi.org/10.2217/iim.12.13
17. Schuhbaeck A, Achenbach S, Layritz C et al (2013) Image quality of ultra-low radiation exposure coronary CT angiography with an effective dose < 0.1 mSv using high-pitch spiral acquisition and raw data-based iterative reconstruction. Eur Radiol 23:597–606. https://doi.org/10.1007/s00330-012-2656-2
18. Halliburton SS, Abbara S, Chen MY et al (2011) SCCT guidelines on radiation dose and dose-optimization strategies in cardiovascular CT. J Cardiovasc Comput Tomogr 5:198–224. https://doi.org/10.1016/j.jcct.2011.06.001